Using SUV as a Guide to ^{18}F-FDG Dose Reduction

David W. Cheng[1], Devrim Ersahin[2], Lawrence H. Staib[2], Daniele Della Latta[3], Assuero Giorgetti[4], and Francesco d'Errico[2]

[1]Sidra Medical and Research Center, Department of Diagnostic Imaging, Doha, Qatar; [2]Yale University School of Medicine, Department of Diagnostic Radiology, New Haven, Connecticut; [3]Fondazione Toscana Gabriele Monasterio per la Ricerca Medica e di Sanità Pubblica, CNR–Regione Toscana, Massa, Italy; and [4]Fondazione Toscana Gabriele Monasterio per la Ricerca Medica e di Sanità Pubblica, CNR–Regione Toscana, Pisa, Italy

This article explores how one can lower the injected ^{18}F-FDG dose while maintaining validity in comparing standardized uptake values (SUVs) between studies. Variations of the SUV within each lesion were examined at different acquisition times. **Methods:** Our protocol was approved by either the Human Investigation Committee or the Institutional Review Board. All 120 PET datasets were acquired continuously for 180 s per bed position in list mode and were reconstructed to obtain 30-, 60-, 90-, 120-, 150-, and 180-s-per-bed-position PET images with registration to a single set of nondiagnostic CT images. Qualitative assessment of the images was performed separately for correlation. The SUV measurements of each lesion were computed and normalized to the 180-s acquisition values to create a stabilization factor. These stabilization factors were used to demonstrate a predictable trend of stabilization over time. The variances of the stabilization factors over the entire dataset, composed of several tumor types over a range of sizes, were compared for each time point with the corresponding 150-s time point using a 2-sided F test, which has similar values to the 180-s time point. **Results:** The variance of the data decreased with increasing acquisition time and with increasing dose but leveled off for sufficiently long acquisitions. **Conclusion:** Through the statistical analysis of SUVs for increasing acquisition times and visual evaluation of the plots, we developed and hereby propose an algorithm that can be used to seek the maximum reduction in administered ^{18}F-FDG dose while preserving the validity of SUV comparisons.

Key Words: ^{18}F-FDG; dose reduction; standardized uptake value; SUV; acquisition time

J Nucl Med 2014; 55:1998–2002
DOI: 10.2967/jnumed.114.140129

It is amply documented that ionizing radiation, such as x-rays in diagnostic imaging, can contribute to the risk of carcinogenesis in humans (*1*). Given the steady and steep rate of increase in the number of CT scans in recent years (*2*), this technique has been the main focus of dose evaluation and dose reduction studies.

With the advent of hybrid imaging, that is, PET/CT and SPECT/CT techniques, dose reduction efforts have initially focused on the CT portion of the scans (*3,4*). Investigators examining radiation exposure in PET/CT imaging estimated the contribution from the CT component to be 54%–81% (*3*), depending on the techniques demanded from the x-ray tube. Published dose reduction studies have focused on minimizing the dose from the CT portion in an effort to achieve a good-quality PET/CT scan with a total effective dose below 10 mSv (*5*). Other studies have explored the effects of various CT techniques on the reconstructed PET images of various phantoms (*6,7*). In these studies, the adequacy of the CT technique yielding the lowest dose exposure was determined qualitatively by clinicians looking for disease on the PET images (*8,9*).

Recently, attention has begun to shift to the contribution from radionuclides to the total radiation dose per scan, since some nuclear medicine procedures may yield doses comparable to the effective dose from CT (*10*). In particular, Alessio et al. (*8*) have suggested a reduction of the positron emitter dose in PET as an alternative to a reduction in CT scanning time in an evaluation based on subjective adequacy and objective lesion detection accuracy by body region. More recently, some studies have suggested an optimization of injected dose based on noise-equivalent count rates (*7,11*). In this approach, radioactivity at the maximum noise-equivalent count rate was defined as an optimal injection dose per unit weight, guided by visual assessment of the images of anthropomorphic phantoms and of patients to meet the criteria of acceptability for the technique. In clinical practice, although staging and restaging from qualitative assessment alone may be adequate, consistency in quantitation, namely the widely used standardized uptake value (SUV), plays an important role in the evaluation of response to therapy. Practitioners rely heavily on changes in SUVs over time, in the absence of clear improvement or progression of disease by detection of previous lesions or new lesions, respectively, to decide whether to continue or switch therapies. We have been reluctant to lower our ^{18}F-FDG dose without exploring the effects on our quantitation. Strobel et al. have found a statistically significant difference in a comparison between 2- and 3-dimensional acquisitions with a 50% reduction in scan time. They demonstrated a 5.2% reduction in maximum SUV (SUV_{max}) using their 3-dimensional protocol without noting significant diagnostic differences visually from the images (*12*).

In this study, we propose a novel approach to dose reduction that differs from earlier ones in that we determined the appropriate dose reduction by searching for the acquisition time at which SUVs become stable. This method preserves valid direct quantitative comparisons between current and previous ^{18}F-FDG PET scans. Furthermore, it may provide a more conservative parameter in determining image quality. We have tested this approach on various tumor types and sizes.

MATERIALS AND METHODS

This effort was initially performed at Yale New Haven Hospital (YNHH) and was later joined by collaborators at the Fondazione

Received Mar. 13, 2014; revision accepted Oct. 27, 2014.
For correspondence or reprints contact: David W. Cheng, Sidra Medical and Research Center, P.O. Box 26999, Doha, Qatar.
E-mail: dcheng@sidra.org
Published online Nov. 11, 2014.

TABLE 1
Demographics of Patients Examined in Each Phase of This Study

Demographic	Phase 1 (555 MBq) YNHH	Phase 2 (370 MBq) YNHH	Phase 2 (3.7 MBq/kg) CNR/FTGM
Sex (F/M)	25/26	25/18	14/12
Age (y)	56.5 ± 18.8 (13–85)	63.2 ± 14.1 (20–92)	60.8 ± 13.4 (23–79)
Body mass index (kg/m^2)	29.0 ± 8.5 (16.4–62.0)	27.5 ± 6.6 (16.3–47.8)	25.7 ± 3.9 (19.5–31.1)
Dose			
mCi	15.1 ± 1.7 (10.7–19.2)	10.4 ± 0.9 (8.4–12.9)	8.2 ± 1.3 (5.4–10.6)
MBq	559 ± 62.8 (396–711)	383 ± 34.9 (311–478)	303 ± 49.1 (201–392)
Dose/kg			
mCi/kg	0.21 ± 0.07 (0.08–0.39)	0.14 ± 0.03 (0.09–0.23)	0.11 ± 0.01 (0.10–0.16)
MBq/kg	7.8 ± 2.4 (3.1–14.4)	5.2 ± 1.3 (3.3–8.5)	4.1 ± 0.5 (3.6–5.8)
Blood glucose (mg/dL)	117.5 ± 30.2 (57–226)	110.7 ± 16.3 (76–153)	100.7 ± 10.6 (77–136)
Uptake time (min)	67.7 ± 10.3 (54–107)	66.4 ± 8.0 (50–91)	63.6 ± 7.7 (56–80)

Data are average ± SD, followed by range in parentheses.

Toscana Gabriele Monasterio per la Ricerca Medica e di Sanità Pubblica CNR–Regione Toscana Pisa (CNR/FTGM). At CNR/FTGM, we had the resources to extend the acquisition time to 240 s per field of view. Our protocol was approved by either the Human Investigation Committee or the Institutional Review Board at both institutions.

The study was structured in 2 phases. The first phase, performed at YNHH only, included the retrospective analysis of 51 consecutive PET/CT studies with a prescribed dose of 555 MBq (15 mCi) of ^{18}F-FDG. In the second phase, 69 consecutive studies (43 at YNHH and 26 at CNR/FTGM) were evaluated using the same protocol as in the first phase, but the prescribed dose was 370 MBq (10 mCi) at YNHH and 3.7 MBq/kg (0.1 mCi/kg) at CNR/FTGM. Also, in the second phase, only patients with diagnoses of breast carcinoma, lymphoma, pancreatic carcinoma, and lung cancer with positive findings were included. Age, sex, body weight, body mass index, administered radiotracer dose, uptake time, blood glucose levels at the time of injection, and diagnoses were recorded (Tables 1 and 2).

The images were acquired using 64-slice PET/CT Discovery 690 scanners (GE Healthcare) at both sites. The hybrid PET/CT Discovery 690 scanner is equipped with a lutetium-yttrium-orthosilicate detector and a 64-slice CT component. The D690 PET scanner operates only in 3-dimensional mode. It consists of 24 rings of detectors (13,824 lutetium-yttrium-orthosilicate crystals total) for an axial field of view of 157 mm; the transaxial field of view is 70 cm. The CT component of the D690 system is a LightSpeed VCT with 912 channels × 64 rows (*13*). Images were reconstructed following our clinical protocol on an AW workstation (GE Healthcare) equipped with version 4.5 software using ordered-subsets expectation maximization with 2 iterations, 24 subsets, and a gaussian z-mm filter. To have a wider acceptance of this application, time-of-flight data were not used in this study.

All PET datasets were obtained by following our standard protocol of a continuous 180 s per bed position, except that they were acquired in list mode and, for our research project purposes only, were reconstructed to obtain 30-, 60-, 90-, 120-, 150-, and 180-s-per-bed-position PET images with registration to a single set of nondiagnostic CT images. CT images were obtained using 120 kVp and sliding amperage. Images were transferred to an AW workstation. All 6 sets of images for each patient were evaluated by 2 board-certified nuclear medicine physicians at each site, who were aware of the clinical diagnoses. Images of the 180-s-per-bed-position data were evaluated first to determine overall findings and the total number of lesions to be measured.

The same data analysis was performed in the 2 phases of the study. In patients with several ^{18}F-FDG–avid lesions, a maximum of 5 lesions presenting well-defined anatomic borders and clear separation from other lesions were selected at random. Lesion sizes were measured in 2 dimensions (maximum and minimum axes) on axial images. SUVs were measured by creating a voxel of interest (VOI) using a fixed threshold of 42% on each lesion on the 180-s image and left at a fixed value. VOIs were checked on all planes (axial, coronal, and sagittal) to ensure that the borders were appropriate for accurate quantitation. Average SUV and SUV_{max} were measured for each lesion at each time point using the 180-s VOI. Cases of focal uptake without corresponding anatomic abnormalities were excluded because of the indeterminate anatomy of the lesions.

TABLE 2
Distribution of Diagnoses and Lesion Sizes in Each Phase of This Study

Diagnosis	Phase 1 (555 MBq) YNHH	Phase 2 (370 MBq) YNHH	Phase 2 (3.7 MBq/kg) CNR/FTGM
Lymphoma	1.4 ± 0.5 cm (0.5–2.4 cm), n = 17	1.3 ± 0.5 cm (0.6–2.5 cm), n = 10	1.2 ± 0.8 cm (0.6–2.7 cm), n = 6
Lung cancer	1.0 ± 0.4 cm (0.6–1.8 cm), n = 8	1.7 ± 0.7 cm (0.7–4.0 cm), n = 19	1.7 ± 0.8 cm (0.7–3.5 cm), n = 18
Breast cancer	2.2 ± 1.3 cm (0.5–4.3 cm), n = 4	1.4 ± 0.5 cm (0.8–2.9 cm), n = 12	1.8 ± 1.3 cm (0.9–2.7 cm), n = 2
Pancreas cancer	1.8 ± 0.7 cm (1.2–2.8 cm), n = 3	1.3 ± 0.9 cm (0.8–2.8 cm), n = 2	Not applicable
Miscellaneous	1.4 ± 1.0 cm (0.4–4.5 cm), n = 19	Not applicable	Not applicable

Data are average ± SD, followed by range in parentheses.

TABLE 3
Perceived Quality of PET Images (51 Scans) from Phase 1 of This Study (Prescribed ^{18}F-FDG Dose, 555 MBq [15 mCi]) as Function of Acquisition Time

Acquisition time (s)	Uninterpretable (%)	Poor (%)	Adequate (%)	Unequivocal %
30	65	29	6	0
60	14	45	41	0
90	0	22	60	18
120	0	2	23	75
150	0	0	6	94
180	0	0	0	100

We expect the stabilization factor to tend to 1 as the acquisition time increases. To demonstrate a predictable trend of stabilization between patients and tumor types over a range of sizes at each time point, the variance of the stabilization factors was computed for all lesions (SUVs normalized to the 180-s acquisition values). The variances were compared with the corresponding 150-s time point using a 2-sided F test. The statistical analysis was performed using the software package "R" (var.test; R Foundation for Statistical Computing).

RESULTS

Maximum-intensity projection and coronal PET images for each data point were qualitatively evaluated and graded as uninterpretable (very noisy image because of paucity of counts), poor (lesion-to-background ratio too low), adequate (difficult but may have a sufficient target-to-background ratio for experienced interpreters), or unequivocal (good lesion-to-background uptake ratio for most interpreters). As shown in Tables 3 and 4, the perceived image quality improves with longer acquisitions.

In both phases of the study, most scans were deemed adequate or unequivocal in quality for interpretation at 120 s of acquisition time. All scans were adequate or unequivocal in quality at 150 s. The perceived improvement in the quality of the scans, as indicated by the shift in percentages within Tables 3 and 4, correlated with lower variance in SUV_{max}, which eventually stabilized on individual plots (Figs. 1–3).

Because of the logistics of ordering ^{18}F-FDG doses, the results from YNHH are based on fixed dosing of either 555 MBq (15 mCi) per patient, that is, our initial protocol, or 370 MBq (10 mCi) per patient, that is, our revised protocol. Given the wide range of body masses of our patients, there was a resultant wide range of 3.3–8.5 MBq (0.09–0.23 mCi)/kg. Our colleagues in Pisa transitioned from unit ^{18}F-FDG dosing at the beginning to a prescribed dose of 3.7 MBq (0.1 mCi)/kg using an Intego automatic ^{18}F dispensing and injecting system (Medrad Europe B.V.).

As can be seen from Figures 1–4, the results from 2 independent series performed at both centers follow the same trend. The consistency of the 2 series demonstrates that the results are reproducible and indicates that the interobserver variability is insignificant. Furthermore, the rate (or slope) of stabilization appears more rapid at higher doses per unit weight, with increasingly smaller deviation of the SUVs obtained at 180 s but not significantly different after 120 s of acquisition time for all injected doses. Indeed, as shown in Table 5, the variance of the data tends to decrease with an increase in acquisition time and dose but levels off for sufficiently long acquisitions. Table 5 also presented the *P* values for the variance of the normalized SUVs compared with the 150-s time point. We have compared with the 150-s time point because the data have been normalized to the 180-s time point. The observed trends suggested the opportunity to switch from 555 MBq (15 mCi) per patient (phase 1) to 370 MBq (10 mCi) per patient (phase 2).

Data from YNHH were constrained to our standard 180 s of scanning time. Conversely, data from CNR/FTGM extend to 240 s of acquisition. When normalized to the 180-s time point, data from CNR/FTGM show some scatter (Fig. 3); such a range of fluctuation is expected from statistical uncertainty inherent within the modality and is within acceptable limits.

DISCUSSION

Although the benefits of administering a lower dose may be intuitive, its effects on quantification may not be immediately realized. Our data demonstrate that the SUV_{max} for each lesion stabilizes with longer acquisitions up to a point beyond which there is no further meaningful improvement (i.e., it has reached a plateau), independent of diagnosis or the size of each lesion. We

TABLE 4
Perceived Quality of PET Images (69 Scans) from Phase 2 of This Study (Prescribed ^{18}F-FDG Dose, 370 MBq [10 mCi] or 3.7 MBq [0.1 mCi]/kg) as Function of Acquisition Time

Acquisition time (s)	Uninterpretable (%)	Poor (%)	Adequate (%)	Unequivocal (%)
30	93	7	0	0
60	51	40	9	0
90	2	60	33	5
120	0	12	60	28
150	0	0	21	79
180	0	0	0	100

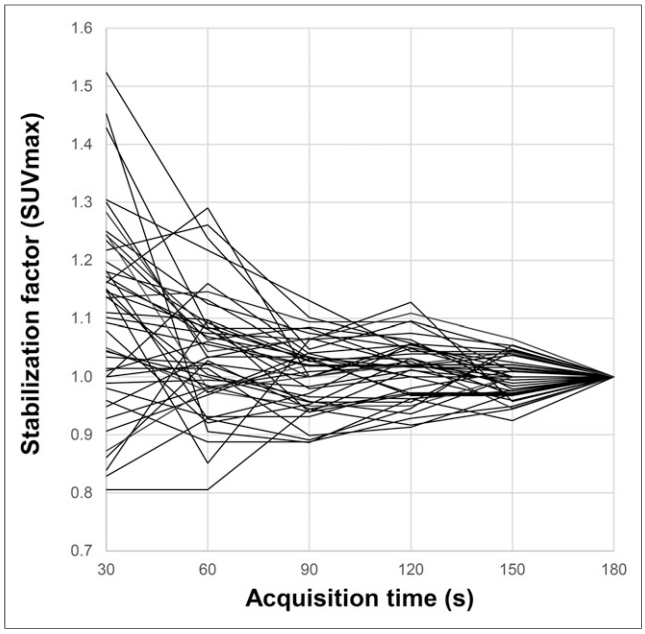

FIGURE 1. Temporal evolution of individual SUVs measured at YNHH for injected ^{18}F-FDG doses of 3.3–4.8 MBq/kg (0.10–0.13 mCi/kg). SUV data are normalized to 180-s time point.

used this critical point to determine how much the dose can be reduced while maintaining consistency in quantification.

Since the inception of PET/CT imaging at YNHH, our dose reduction efforts have incorporated the use of a very low dose nondiagnostic CT technique for attenuation correction. Because our oncologist colleagues use changes in SUV as a part of their assessment of response to therapy, we have to explore the effects of a major change in our protocol on the precision of our quantitation. We expected that a quantitative parameter would be more sensitive

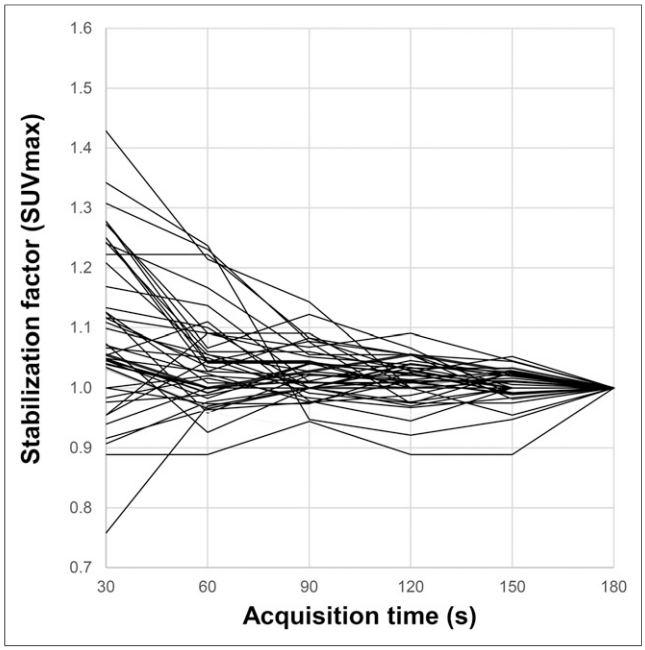

FIGURE 2. Temporal evolution of individual SUVs measured at YNHH for injected ^{18}F-FDG doses of 5.2–8.5 MBq/kg (0.14–0.2 mCi/kg). SUV data are normalized to 180-s time point.

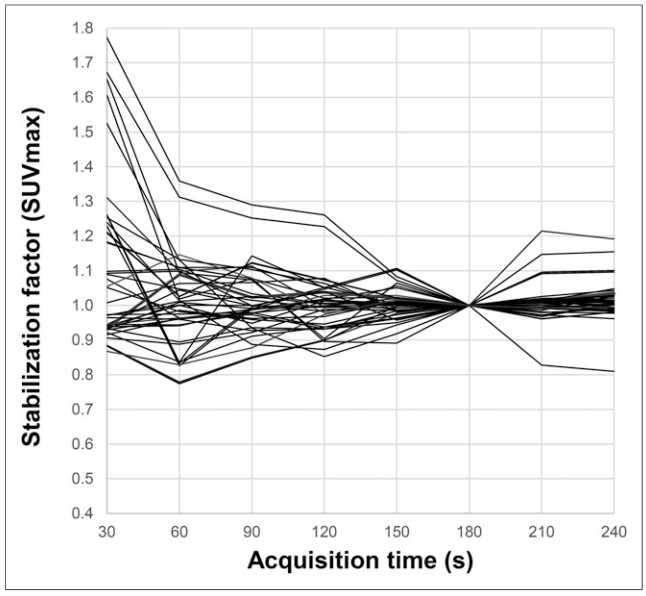

FIGURE 3. Temporal evolution of individual SUVs measured at CNR/FTGM for injected ^{18}F-FDG doses of 4.4–4.8 MBq/kg (0.12–0.13 mCi/kg). SUV data are normalized to 180-s time point.

than the human eye in evaluating changes in the image and would ensure confidence in longitudinal comparisons.

We chose to focus on the determination of SUV_{max}, rather than average SUV, to avoid effects from arbitrary margin selection of the VOI by vendor software and from the heterogeneity of uptake within each lesion. Because each lesion served as its own control over a range of 180–240 s of acquisition time, which is very short compared with the 60 min between injection time and imaging for biodistribution, ^{18}F-FDG avidity and partial-volume effects will be properties intrinsic to each lesion during the course of assessment. We limited the number of lesions to be selected from each patient to restrict biases due to differences in biodistribution from any particular patient with the same diagnosis in our grouped analyses. After analyzing the results from our early protocol using 555 MBq (15 mCi) of ^{18}F-FDG, we confidently lowered our fixed dose to 370 MBq (10 mCi), noting that similar results can be obtained through trimming the imaging time or the administered dose.

The simplicity of our approach lies in comparing each lesion with itself, measured after the same time for biodistribution and

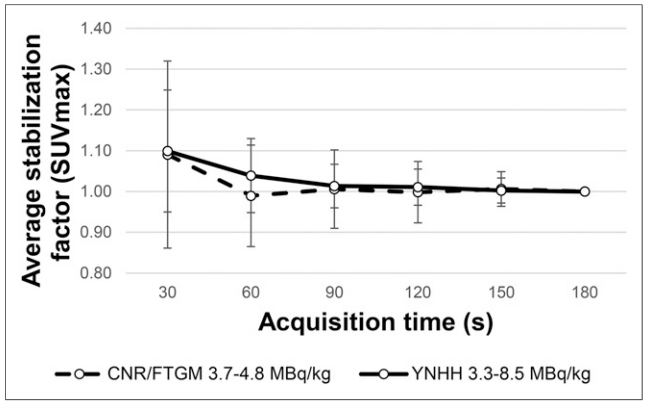

FIGURE 4. Temporal evolution of all SUVs collectively. Individual SUV at each time point was normalized to SUV at 180-s time point in each group, before determination of SD.

TABLE 5
SD and *P* Values for Variance of Normalized SUV_{max} of All Plots Within Each Subcategory of Acquisition Time and Dose Range

	Dose							
	3.3–4.1 MBq/kg (0.09–0.11 mCi/kg)		4.4–4.8 MBq/kg (0.12–0.13 mCi/kg)		5.2–5.6 MBq/kg (0.14–0.15 mCi/kg)		5.9–8.5 MBq/kg (0.16–0.23 mCi/kg)	
Acquisition time (s)	σ	*P*	σ	*P*	σ	*P*	σ	*P*
30	0.18	1.0E−11	0.15	3.0E−9	0.15	2.0E−16	0.11	1.0E−5
60	0.11	8.0E−8	0.09	0.0001	0.08	6.0E−11	0.07	0.004
90	0.05	0.02	0.06	0.04	0.05	6.0E−6	0.04	0.99
120	0.05	0.01	0.05	0.29	0.04	0.001	0.04	0.8
150	0.03		0.04		0.02		0.04	

maintaining the same intrinsic properties, including partial-volume effects. Hence, the variability in the measurements comes from only the counting statistics within the VOI. As can be seen in Figure 4, SUV_{max} is most overestimated with the fewest counts from the shortest acquisition time. The deviation is skewed above unity because of the way SUV is quantified.

In our early protocol using 555 MBq (15 mCi) of ^{18}F-FDG, the rate of stabilization plateaued within 120 s of acquisition time regardless of tumor type and size (Fig. 2). These findings gave us the confidence that we could trim our dose by one third while maintaining our acquisition time of 180 s per bed position.

We introduced a protocol using 370 MBq (10 mCi) of ^{18}F-FDG and monitored its performance to ensure that we achieved good precision through adequate counting statistics. Our team in Pisa verified these findings independently and provided invaluable additional data with 240 s of acquisition time at 370 MBq (10 mCi) of ^{18}F-FDG. It was reassuring that the variability between 180 and 240 s of acquisition was within 10% (Figs. 1 and 3). The shape of the curve suggests that there may be room for further reduction in the ^{18}F-FDG dose.

Although our approach is scientifically based, one limitation of this study is that it has been tested only on GE Healthcare PET/CT scanners using their standard clinical reconstruction parameters. Further studies using scanners from other vendors and optimization of the reconstruction parameters to vary the noise level of the data can strengthen the confidence and validity of this approach. Given the variety of tumor types and sizes in our study, we are confident that the behavior of the graphs will remain predictable until the noise level of the data dominates over the true counts.

CONCLUSION

Using an objective quantitative parameter that is more precise and likely more sensitive than qualitative assessment alone, we have introduced a simple, direct, and practical approach to evaluate the effect that reducing the ^{18}F-FDG dose has on imaging, to enhance our confidence in comparing longitudinal ^{18}F-FDG PET studies. Comparing each lesion with itself at different time points in a continuous acquisition allows all factors such as the intrinsic characteristics of the scanner, biodistribution time, diagnosis, and size to remain constant.

We feel that our approach complements existing methods and can easily be adopted in clinical practice. These efforts will lead to lower cumulative doses and will benefit patients, especially children, who may require multiple PET/CT or SPECT/CT studies over their lifetime.

DISCLOSURE

The costs of publication of this article were defrayed in part by the payment of page charges. Therefore, and solely to indicate this fact, this article is hereby marked "advertisement" in accordance with 18 USC section 1734. No potential conflict of interest relevant to this article was reported.

ACKNOWLEDGMENT

We thank David Menard, CNMT, of YNHH for acquiring the images in list mode and processing the images expertly.

REFERENCES

1. Pearce MS, Salotti JA, Little MP, et al. Radiation exposure from CT scans in childhood and subsequent risk of leukaemia and brain tumours: a retrospective cohort study. *Lancet.* 2012;380:499–505.
2. United Nations Scientific Committee on the Effects of Atomic Radiation. *Sources and Effects of Ionizing Radiation: UNSCEAR 2008 Report to the General Assembly, with Scientific Annexes.* Vol 1. New York, NY: United Nations Publications; 2010:10.
3. Huang B, Li J, Law MW, Zhang J, Shen Y, Khong P. Radiation dose and cancer risk in retrospectively and prospectively ECG-gated coronary angiography using 64-slice multidetector CT. *Br J Radiol.* 2010;83:152–158.
4. Nievelstein RA, van Ufford HQ, Kwee T, et al. Radiation exposure and mortality risk from CT and PET imaging of patients with malignant lymphoma. *Eur Radiol.* 2012;22:1946–1954.
5. Willowson KP, Bailey EA, Bailey DL. A retrospective evaluation of radiation dose associated with low dose FDG protocols in whole-body PET/CT. *Australas Phys Eng Sci Med.* 2012;35:49–53.
6. Fahey FH, Palmer MR, Strauss KJ, Zimmerman RE, Badawi RD, Treves ST. Dosimetry and adequacy of CT-based attenuation correction for pediatric PET: phantom study. *Radiology.* 2007;243:96–104.
7. Inoue K, Kurosawa H, Tanaka T, Fukushi M, Moriyama N, Fujii H. Optimization of injection dose based on noise-equivalent count rate with use of an anthropomorphic pelvis phantom in three-dimensional ^{18}F-FDG PET/CT. *Radiol Phys Technol.* 2012;5:115–122.
8. Alessio AM, Sammer M, Phillips GS, Manchanda V, Mohr BC, Parisi MT. Evaluation of optimal acquisition duration or injected activity for pediatric ^{18}F-FDG PET/CT. *J Nucl Med.* 2011;52:1028–1034.
9. Brix G, Lechel U, Glatting G, et al. Radiation exposure of patients undergoing whole-body dual-modality ^{18}F-FDG PET/CT examinations. *J Nucl Med.* 2005;46:608–613.
10. Jafari ME, Daus AM. Applying Image GentlySM and Image WiselySM in nuclear medicine. *Health Phys.* 2013;104(suppl):S31–S36.
11. Accorsi R, Karp JS, Surti S. Improved dose regimen in pediatric PET. *J Nucl Med.* 2010;51:293–300.
12. Strobel K, Rüdy M, Treyer V, Veit-Haibach P, Burger C, Hany TF. Objective and subjective comparison of standard 2-D and fully 3-D reconstructed data on a PET/CT system. *Nucl Med Commun.* 2007;28:555–559.
13. Bettinardi V, Presotto L, Rapisarda E, Picchio M, Gianolli L, Gilardi M. Physical performance of the new hybrid PET/CT Discovery-690. *Med Phys.* 2011;38:5394–5411.